Molecular Therapy
Nucleic Acids
Original Article

The Aptamer Ob2, a novel AChE inhibitor, restores cognitive deficits and alleviates amyloidogenesis in 5×FAD transgenic mice

Zhiman Liang,[1,2] Xin Li,[1] Xiaoting Luo,[3] Hongjie Luo,[4] Yajun Chen,[4] Mingliang Cai,[3] Xinxin Zhong,[1] Yingying Fang,[1] Ting Guo,[1] Yusheng Shi,[3,5] and Xingmei Zhang[1]

[1]Key Laboratory of Mental Health of the Ministry of Education, Guangdong-Hong Kong-Macao Greater Bay Area Center for Brain Science and Brain-Inspired Intelligence, Guangdong Province Key Laboratory of Psychiatric Disorders, Department of Neurobiology, School of Basic Medical Sciences, Southern Medical University, Guangzhou 510515, China; [2]Department of Pathology, The Fifth Affiliated Hospital, Southern Medical University, Guangzhou 510900, China; [3]Department of Radiation Oncology, Nanfang Hospital, Southern Medical University, Guangzhou 510515, China; [4]The First Affiliated Hospital, Southern Medical University, Guangzhou 510515, China; [5]Department of Radiation Oncology, Zhuhai People's Hospital, Zhuhai Hospital Affiliated with Jinan University, Zhuhai 519000, China

Loss of cerebral cholinergic neurons and decreased levels of acetylcholine (ACh) are considered to be major factors causing cognitive dysfunction in Alzheimer's disease (AD). Abnormally elevated levels of acetylcholinesterase (AChE) resulting in decreased levels of ACh are common in AD patients; thus, AChE inhibitors (AChEIs) are widely used for the treatment of AD. In our previous work, we acquired DNA aptamers Ob1, Ob2, and Ob3 against human brain AChE from systematic evolution of ligands by exponential enrichment (SELEX). In this study, we investigated the effect of these aptamers on learning and memory abilities, as well as the underlying mechanism in a 5×FAD transgenic AD mouse model. Here, we showed that only aptamer Ob2 exhibits a good inhibitory effect on both mouse and human AChE activity. In addition, chronic treatment with aptamer Ob2 significantly improved cognitive ability of 5×FAD mice in the Morris water maze. Moreover, the mechanism of aptamer Ob2 in 5×FAD mice may be associated with its inhibition of AChE activity, alleviation of the levels of Aβ by lowering the expression of β-secretase (BACE1), and activation of astrocytes in the brains of 5×FAD mice. These results indicate that aptamer Ob2 exhibits potential as an effective AChEI for the treatment of AD.

INTRODUCTION

Alzheimer's disease (AD) is the most common type of dementia, characterized clinically by a progressive decline in memory and other cognitive functions, which imposes immense suffering on patients and their families. According to the World Alzheimer Report 2018,[1] worldwide around 50 million people live with dementia, and this number will more than triple to 152 million by 2050. However, the molecular etiology of AD remains unclear. The characteristic features in the brains of AD patients include amyloid plaques (Aβ), tau-protein aggregation, neuroinflammation, loss of cerebral cholinergic neurons, and decreased levels of acetylcholine (ACh).[2–6] Many attempts have been made to develop an effective drug to treat the disease; however, only a few drugs have been approved. Most of these drugs are acetylcholinesterase inhibitors (AChEIs).

Acetylcholine (ACh) is widely distributed in the nervous system, mediates neurotransmission, and plays a critical role in modulating cognitive performance and normal learning and memory processes.[7,8] Basal forebrain cholinergic cell loss is a consistent feature of Alzheimer's disease (AD).[9] Generally, acetylcholinesterase (AChE), which rapidly hydrolyzes ACh, plays a critical role in terminating neurotransmission at cholinergic synapses.[10] Abnormally elevated levels of AChE resulting in decreased levels of ACh are are common in AD patients.[11,12] Therefore, AChEIs, which ameliorate memory and cognitive deficits in AD patients by enhancing central cholinergic neurotransmission, have been widely used for the treatment of mild to moderate AD.

In addition, accumulating evidence suggests that AChE has secondary, noncholinergic functions, including neuroprotection and the processing and deposition of Aβ.[13] AChE could play a role during an early step in the development of amyloid plaques.

Aptamers are single-stranded oligonucleotides screened from a large-capacity random single-stranded DNA (ssDNA) or RNA library by systematic evolution of ligands by exponential enrichment (SELEX).

Received 7 October 2021; accepted 25 February 2022;
https://doi.org/10.1016/j.omtn.2022.02.018.

Correspondence: Xingmei Zhang, Key Laboratory of Mental Health of the Ministry of Education, Guangdong-Hong Kong-Macao Greater Bay Area Center for Brian Science and Brain-Inspired Intelligence, Guangdong Province Key Laboratory of Psychiatric Disorders, Department of Neurobiology, School of Basic Medical Sciences, Southern Medical University, No. 1838 Guangzhou Avenue, Guangzhou 510515, China
E-mail: zhangxm@smu.edu.cn
Correspondence: Yusheng Shi, Department of Radiation Oncology, Nanfang Hospital, Southern Medical University, No. 1838 Guangzhou Avenue, Guangzhou 510515, China
E-mail: syszxm@hotmail.com

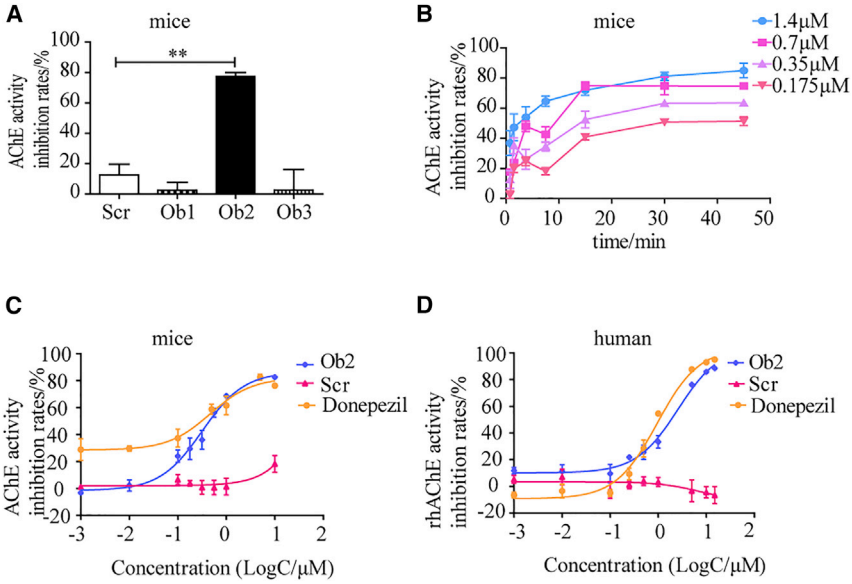

Figure 1. Anti-AChE activity by aptamer Ob2 *in vitro*

(A) Percentage of anti-AChE activity in mouse brain homogenates treated with aptamers Ob1, Ob2, and Ob3 and the control aptamer Scr *in vitro*. **p < 0.01.

(B) Time inhibition curve of mouse brain homogenate AChE activity by different concentrations of aptamer Ob2 *in vitro*.

(C) Concentration inhibition curve of mouse brain homogenate AChE activity by aptamer Ob2, Scr, and positive control drug donepezil *in vitro*.

(D) Concentration inhibition curve of human recombinant (rh)AChE activity by aptamer Ob2, Scr, and positive control drug donepezil *in vitro*.

Due to their three-dimensional structure, aptamers are capable of binding to target molecules, including cells, proteins, peptides, or small molecules, with specificity and high affinity.[14–16] Aptamers also possess several advantages over natural antibodies,[17–19] including ease of synthesis, facile chemical modification, good stability, low toxicity, low immunogenicity, and rapid tissue penetration. These advantages have made aptamers widely used in therapy, diagnostics, and imaging applications.[20–22]

In our previous work, we acquired DNA aptamers Ob1, Ob2, and Ob3 against human brain AChE from SELEX.[23] The 5×FAD mouse model expresses five familial (FAD) mutations, and our previous work has demonstrated that 5×FAD is an effective AD animal model.[24] In this study, we tested the inhibitory effect of these aptamers on the enzyme activity of mouse brain AChE *in vitro*. Then, we detected whether the aptamer could specifically recognize and bind to recombinant human AChE (rhAChE). Furthermore, we examined the symptomatic effects of the aptamer in a 5×FAD-transgenic AD mouse model.

RESULTS

Anti-acetylcholinesterase activity assay in vitro

Aptamers Ob1, Ob2, and Ob3 are three aptamers obtained from previous SELEX against human brain AChE. The *in vitro* inhibitory activities of aptamers Ob1, Ob2, and Ob3 against AChE were determined using an AChE assay kit (A024; Nanjing Jiancheng Bioengineering Institute, Nanjing, China). Scr is a random sequence used as a negative control throughout the experiment. Sequences of aptamers Ob1, Ob2, Ob3 and Scr are shown in Table S1. Similar to aptamer Scr, aptamers Ob1 and Ob3 had no significant inhibitory effect on the AChE activity of mouse brain homogenates (Figure 1A). However, aptamer Ob2 had a significant inhibitory effect on the AChE activity of mouse brain homogenates (Figure 1A). As shown in Figure 1B, mouse brain AChE exposed to different concentrations of aptamer Ob2 at 37°C for 30 min reached the maximum inhibitory effect. As shown in Figure 1C, aptamer Ob2 exhibited anti-AChE activity in mouse brain homogenates in a dose-dependent manner, and the half-maximal AChE inhibition concentration of aptamer Ob2 was 0.32 μM as calculated by linear regression analysis. Donepezil, an effective AChE inhibitor approved by the Food and Drug Administration (FDA), was used as a positive control, and the IC_{50} was 0.47 μM for the inhibition of mouse brain homogenate AChE (Figure 1C). Furthermore, to confirm that aptamer Ob2 exhibits a similar inhibitory effect on rhAChE, we detected rhAChE activity after incubation with different concentrations of aptamer Ob2 or the positive control donepezil. Based on Figure 1D, the IC_{50} of aptamer Ob2 on rhAChE was 2.57 μM, whereas that of donepezil was 0.95 μM. These results indicate that aptamer Ob2 has a good inhibitory effect on both mice and human AChE activity.

Binding affinity measurements of aptamers against RhAChE

Indirect enzyme-linked immunosorbent assay (ELISA) was performed to determine the binding affinity of the aptamer Ob2 to rhAChE. Anti-AChE antibody and unrelated aptamer Scr were used as the controls. Similarly to anti-AChE, the binding curve of aptamer Ob2 to rhAChE fitted well (Figures 2A–2C), with K_d values in the nanomolar range. These findings indicated that aptamer Ob2 can specifically bind to rhAChE with high affinity (K_d = 17.09 ± 9.86 nM). The secondary structures of aptamer Ob1, Ob2, and Ob3 were predicted by the MFOLD program (Figure S1). We observed loops and hairpins from aptamer Ob2, indicating that aptamer Ob2 possessed the ability to bind to special sites of rhAChE.

In vivo assessment of aptamer Ob2's effect on AD mice

The ability of aptamer Ob2 to improve learning and memory deficits in AD mice was evaluated by behavioral research, including the Y maze and the Morris water maze. All mice used in the experiment were 3- to 4-month-old male 5×FAD mice that received repeated intraventricular infusions of NaCl, negative control Scr, or aptamer Ob2, respectively (Figure 3A). The infusion position is shown in Figure 3B. After 15 repeated injections of aptamer, mice were handled for 3 days before behavioral tests. In the open-field test, the total distances

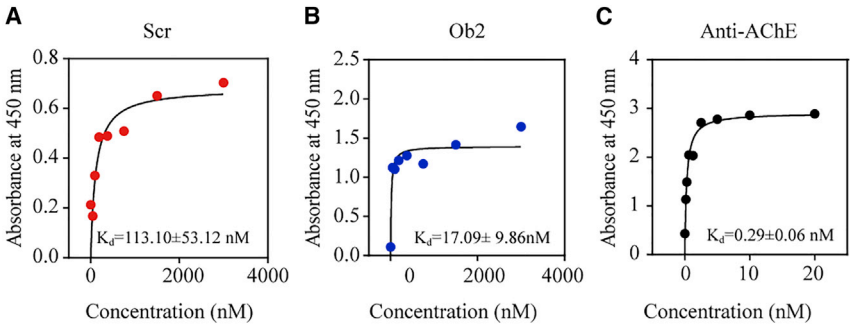

Figure 2. Affinity measurements of aptamer Ob2 against rhAChE

(A–C) Binding curves of unrelated aptamer Scr (A), aptamer Ob2 (B), and anti-AChE (C).

traveled and center times between NaCl-treated group, Scr-treated group, and Ob2-treated group (Figure 3C) were similar (NaCl: n = 12, Scr: n = 10, Ob2: n = 10). In the Y maze, no significant differences in the number of arms entered and spontaneous alternation of the mice (Figure 3D) were noted between the NaCl-treated, Scr-treated, and Ob2-treated groups. The results show that aptamer Ob2 did not improve the working memory of mice. In addition, we then performed the Morris water maze to test the spatial memory of the mice. After treating AD mice with the aptamer Ob2, spatial memory was improved compared with that of Scr-treated and NaCl-treated mice (Figures 4A–4G). These results indicate that the AChE-specific aptamer Ob2 was able to ameliorate the spatial memory of AD mice.

Aptamer Ob2 decreased aβ levels in 5×FAD mice

The synthesis and degradation of amyloid-β (Aβ) is one of the main pathological markers of AD. To investigate whether aptamer Ob2 could alter Aβ levels in the brains of 5×FAD mice, ELISA and immunohistological (IHC) assays were performed. thioflavin-S (ThS) was used to visualize Aβ plaques. Compared with the Scr-treated 5×FAD group, the number or area of plaques in the Ob2-treated 5×FAD group was reduced in the hippocampus (Figure 5A) and cortex (Figure 5B). Consistent with the results from ThS staining, we observed alterations in the levels of Aβ plaques in both the hippocampus (Figures 6A and 6C) and cortex (Figures 6B and 6D) by immunofluorescence using the monoclonal anti-Aβ antibody 6E10. Among the various isomers of Aβ, $Aβ_{40}$ is the major secreted form, and $Aβ_{42}$ is the most amyloidogenic and neurotoxic. Furthermore, we detected total $Aβ_{40}$ and $Aβ_{42}$ levels by ELISA. As shown in Figure 7A, $Aβ_{42}$ in the hippocampus or cortex was decreased with aptamer Ob2 treatment. Similarly, we detected a reduction in the total $Aβ_{40}$ levels (Figure 7B) in the hippocampus or cortex of aptamer Ob2-treated 5×FAD mice. Together, these results indicate that the Aβ burden was decreased by the administration of aptamer Ob2.

Aptamer Ob2 reduced the activation of astrocytes in 5×FAD mice

In AD, reactive astrocytes cluster around Aβ plaques in response to the neural injury associated with Aβ and are accompanied by an increase in the expression of glial fibrillary acidic protein (GFAP). To identify whether aptamer Ob2 has an inhibitory effect on the activation of astrocytes, we evaluated GFAP immunoreactivity (Figures 6A–6C). Our data revealed that aptamer Ob2 treatment decreased GFAP immunoreactivity in the hippocampus or cortex in 5×FAD mice. These results indicated that aptamer Ob2 evidently inhibited the activation of astrocytes in 5×FAD mice.

Aptamer Ob2 regulated the expression of AD-related proteins

Aβ is produced through the sequential cleavage of amyloid precursor protein (APP) by β-site APP-cleaving enzyme 1 (BACE1) and γ-secretase. BACE1 cleavage of APP produces soluble amyloid precursor protein β (sAPPβ). A third anti-amyloidogenic protease, α-secretase, can cleave APP at a site within Aβ and form a soluble N-terminal fragment (sAPPα) to preclude Aβ formation. Our previous results had shown that aptamer Ob2 could decrease the Aβ content. Therefore, we performed western blotting to detect the expression of AD-related proteins. We observed an obvious decrease in BACE1 expression in the hippocampus (Figures 8A and 8B) and cortex (Figures 8C and 8D) after 5×FAD mice were treated with Ob2. Moreover, sAPPβ was also decreased in the hippocampus (Figures 8A and 8B) and cortex (Figures 8C and 8D). However, no significant decrease in sAPPα expression was noted in the hippocampus (Figures 8A and 8B) or cortex (Figures 8C and 8D). Therefore, as an AChE inhibitor, aptamer Ob2 was able to influence the APP processing and decrease Aβ deposition.

DISCUSSION

To date, AChEIs remain the first-line symptomatic therapeutic approach for AD. Studies have demonstrated that AChE participates in AD neurodegenerative progression. AChE accelerates the assembly of Aβ into amyloid fibrils. AChEIs could act through a cholinergic pathway by increasing the levels of the neurotransmitter ACh at the synapse, compensating for the central cholinergic deficit characteristic of AD. Moreover, AChEIs could interfere with APP processing through inhibition of BACE1 (β-secretase) and γ-secretase, which are involved in the formation of Aβ.[25] The three AChEIs currently aprroved by the FDA are donepezil, rivastigmine, and galantamine. All are considered first-line symptomatic treatments of the various phases of AD and may even have potentially disease-modifying effects. These AChEIs used in different dosages for mild to severe AD can cause severe side effects including bradycardia and orthostatic hypotension, diarrhea, vomiting, nausea, fatigue, insomnia, loss of appetite, and weight loss. Tacrine was the first AChEI aprroved by the FDA for the treatment of mild or moderate AD, but due to its hepatotoxicity its use was discontinued. Furthermore, these AChEIs have short half-lives and usually have a brief period of effectiveness.

Aptamers Ob1, Ob2, and Ob3 are three aptamers obtained from previous SELEX against human brain AChE. Our *in vitro* studies

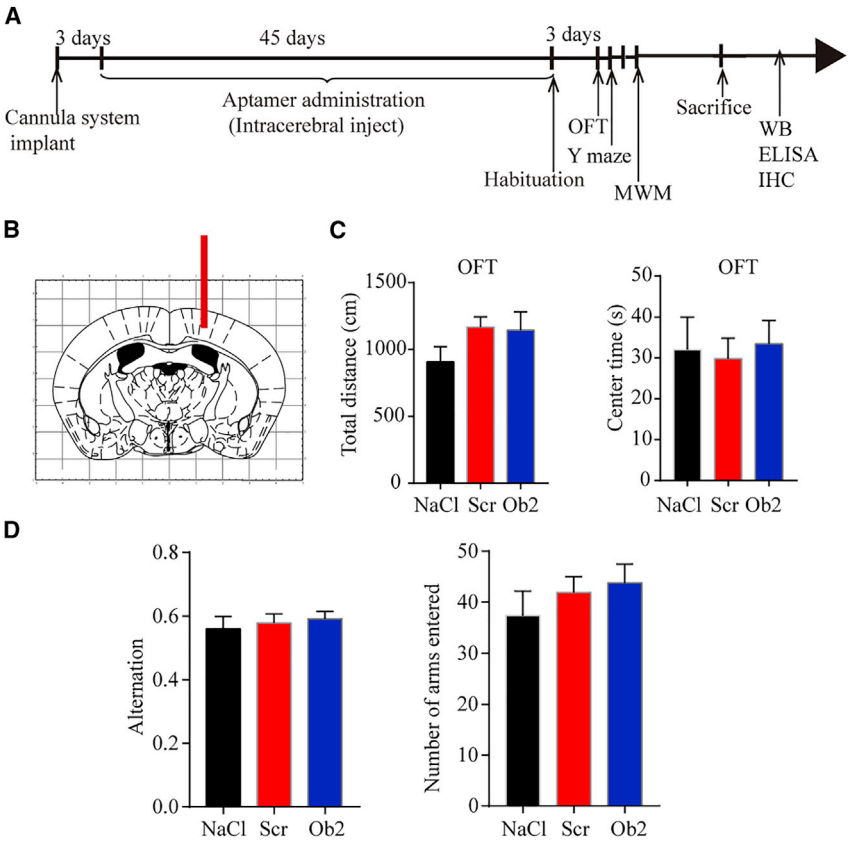

Figure 3. Effects of aptamer Ob2 on exercise capacity and working memory in transgenic 5×FAD mice after intracerebral administration

(A) Schematic timeline of drug treatment and behavioral test order in 5×FAD mice. OFT, open-field test; MWM, Morris water maze; IHC, immunohistochemistry.

(B) Illustration of the indwelling cannula system implanted site (adapted from "The mouse brain in stereotaxic coordinates" Paxinos and Franklin 2004).

(C) Total distance traveled and time spent in center area in total 5 min in OFT (NaCl: n = 12, Scr: n = 10, Ob2: n = 10).

(D) Spontaneous alternation (left) and number of arms entered (right) in the Y maze. (NaCl: n = 12, Scr: n = 10, Ob2: n = 10)

confirmed that aptamer Ob2 has a high affinity for AChE and inhibits AChE activity. In addition, this study showed that aptamer Ob2 exerted a disease-modifying effect in a mouse model of AD. Treatment of 5×FAD mice with the aptamer Ob2 effectively improved cognitive ability and memory dysfunction compared with treatment of these mice with the random aptamer Scr.

Aβ in the brain is highly correlated with memory-related synaptic dysfunctions in AD. Many studies support the hypothesis that increased Aβ brain levels caused by overproduction of and failure to clear this peptide is the initiating factor for the pathological cascade ultimately leading to dementia in AD.[26–28] To further investigate the mechanism by which aptamer Ob2 improves cognitive ability and memory dysfunction in AD model mice, we later performed histopathological and biochemical analyses. In this study, IHC staining and ThS staining results demonstrated that aptamer Ob2 significantly decreased Aβ plaques. In addition, aptamer Ob2 significantly reduced the total Aβ levels detected by ELISA. BACE1 cleavage of APP produces sAPPβ, and α-secretase cleaves APP at a site within Aβ and sAPPα to preclude Aβ formation.[29,30] Western blotting results indicated that aptamer Ob2 reduced the expression of BACE1 in 5×FAD mice, followed by its product sAPPβ, which was decreased as well. However, there was no significant decrease in sAPPα expression. These results indicated that aptamer Ob2 could alleviate brain Aβ levels by reducing the expression of BACE1 in 5×FAD mice.

In addition, reactive astrocytes are integral components of neuritic plaques in AD model mice and in AD human brains.[31] Therefore, to clarify the effect of aptamer Ob2 on Aβ deposition-induced glial activation in 5×FAD mice, we performed IHC staining of brain tissue with astrocyte-specific antibodies. Our results indicated that astrocyte activation was reduced following aptamer Ob2 treatment.

Many studies have reported that AChE can be used as a disease predictor. For example, AChE is a promising independent prognostic predictor for hepatocellular carcinoma (HCC) recurrence and the survival of HCC patients.[32] Blood AChE levels are a potential biomarker for the early detection of cerebral amyloid deposition in cognitively normal individuals.[33] Monoclonal antibodies specific for AChE could be used in the prenatal diagnosis of neural tube defects.[34] These studies suggest that we can further study the potential of aptamer Ob2 as a predictor of early AD.

On the basis of the diversity and multiplicity of the pathogenetic elements of AD, it is not sufficient to effectively treat AD by applying single putative therapeutic agents. Therefore, dual- or multitarget drugs that simultaneously act on different AD targets or mechanisms of pathogenesis are thought to be beneficial for AD treatment.[35,36] Our study found that aptamer Ob2 effectively improved cognitive ability and memory dysfunction in 5×FAD mice by inhibiting AChE and interfering with Aβ. Therefore, we hypothesized that aptamer Ob2 is a dual-binding-site AChEI. Aptamers are single-stranded DNA or RNA oligonucleotides that fold into specific 3D structures and bind to specific target molecules with high affinity and specificity. Aptamers have made some progress in the treatment of brain diseases.[37–39] However, aptamers are susceptible to exonucleases and endonucleases in blood. Aptamers can undergo chemical modification to modulate their pharmacokinetic profile, including conferring nuclease resistance and increasing circulating half-life. These characteristic of aptamers made them a good choice for development of a new AChEI for the therapy of mild to severe AD.

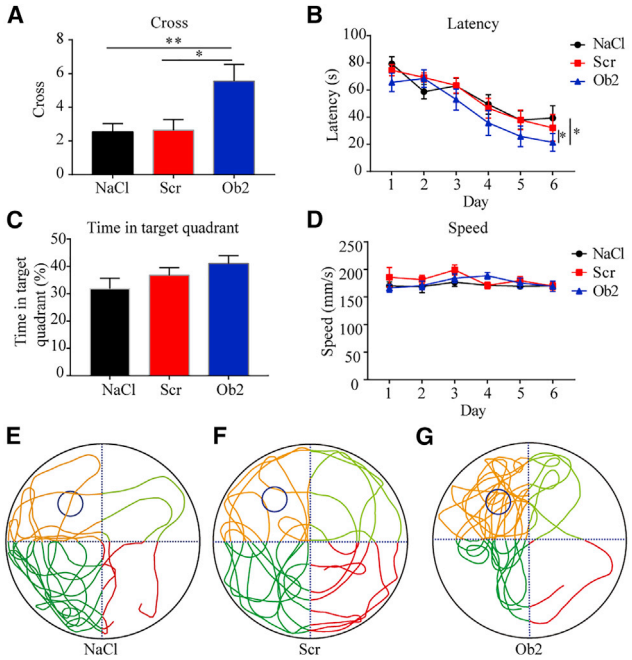

Figure 4. Improvement of spatial learning and memory ability in the water maze of 5×FAD mice after intracerebral administration of aptamer Ob2

(A) Number of target location crossings during the probe test. **$p < 0.01$, *$p < 0.05$.

(B) Latency to reach hidden platform in the training phase. *$p < 0.05$.

(C) Percentage of time spent in the target quadrant in the probe test.

(D) Average swimming speed in the training phase.

(E–G) Representative traces in the probe test of the Morris water maze. (NaCl: n = 12, Scr: n = 10, Ob2: n = 10).

In conclusion, this paper offers essential preclinical evidence that the dual-binding-site AChEI aptamer Ob2 can improve learning and memory dysfunction in 5×FAD-transgenic mice. Its mechanisms of action may include the following three aspects: (1) increase the concentration of neurotransmitter ACh by inhibiting AChE, (2) alleviate brain Aβ levels by reducing the expression of BACE1, and (3) ameliorate astroglial reactivity.

MATERIALS AND METHODS

Animals

All experiments were performed using male 5×FAD mice (no. 008730; Jackson Laboratories, Bar Harbor, ME), at 4 months of age at the beginning, that harbor five FAD mutations in amyloid precursor protein (APP) and presenilins (PS1) on the C57/B6XSJL background. The mice were identified via a PCR instrument from Bio-Rad (T100 Thermal Cycler), using DNA from mouse tails. The mice were housed in a room under controlled temperature (21–25°C) with an alternating 12-h light/12-h dark cycle and free access to food and water. Behavioral tests were performed during the light cycle between 12:00 and 19:00 in a sound-attenuated and air-regulated experimental room and with at least 30 min of habituation before the behavioral tests. All experiments were performed in accordance with the Chinese Council on Animal Care Guidelines and were approved by the Southern Medical University Animal Ethics Committee.

Aptamer synthesis

Aptamers Ob1, Ob2, and Ob3 are aptamers for human brain AChE. Our previous results indicated that aptamers Ob1, Ob2, and Ob3 can specifically recognize human brain AChE without cross-reaction with erythrocyte AChE.[23] Aptamers Ob1, Ob2, Ob3, and Scr were synthesized by Invitrogen (Carlsbad, CA). Aptamers were diluted to a suitable concentration in 0.9% saline solution. The aptamers were heated at 95°C for 5 min, snap-cooled on ice for 5 min, and maintained at room temperature (RT) for 10 min prior to the treatment of each experiment.

Detection of AChE activity assay

For *in vitro* inhibition studies, mice were euthanized using carbon dioxide (CO_2) and cervical dislocation. The cerebral tissue was rapidly removed and washed with ice-cold saline to remove blood from the surface of the cerebral tissue. Brain tissues were homogenized thoroughly with a mechanical homogenizer in nine volumes of saline (w/v). The homogenates were centrifuged at 3,000 rpm at 4°C for 10 min. The supernatant was collected, and the protein concentration was determined using a BCA assay kit (23,227; Thermo Fisher Scientific). Then, the supernatant was preincubated with the same volume of different concentrations of aptamers Ob1, Ob2, Ob3, negative control aptamer Scr, or positive control donepezil for 30 min at 37°C followed by measurement of residual AChE activities. The mixture (5 μL per well) or mouse supernatant (2.5 μL per well) was added to a 96-well plate as the detected sample. AChE enzyme activities were assayed using an AChE assay kit (A024; Nanjing Jiancheng Bioengineering Institute, Nanjing, China) according to the method of Ellman, with slight modifications,[40] and all samples were determined in duplicate. Enzymatic activity was determined by measuring the optical density (OD) at 412 nm in a Victor X32,030 multilabel plate reader (PerkinElmer, Waltham, MA, USA) and expressed as micromoles per milligram per minute of protein. AChE inhibition rates (%) were compared with brain tissue homogenates without any treatment. Seven inhibitor concentrations were used in triplicate to construct concentration-response curves using GraphPad Prism 7.0, which enabled interpolation of IC_{50} values.

Binding affinity assay

RhAChE (6.19 nM per well, diluted in 1× PBS) was coated onto 96-well plates at 4°C overnight. The wells were then washed three times with PBST (0.01% Tween 20 in 1× PBS, pH 7.4) and blocked with 5% BSA in 1× PBS at 37°C for 60 min. After three washes with PBST, 50 μL of denatured biotinylated aptamers of different concentrations were added into each well and incubated at 37°C for 60 min. After three washes with PBST, streptavidin-conjugated horseradish peroxidase (50 μL, 1:1,000 in PBS; Sigma-Aldrich, St. Louis, MO, USA) was added to the wells, and incubation was carried out at 37°C for 2 h. Washing was performed three times with PBST, 50 μL of TMB (P0209; Beyotime Biotechnology, Shanghai, China) solution was added, and incubation was carried out for 30 min at RT. The reaction

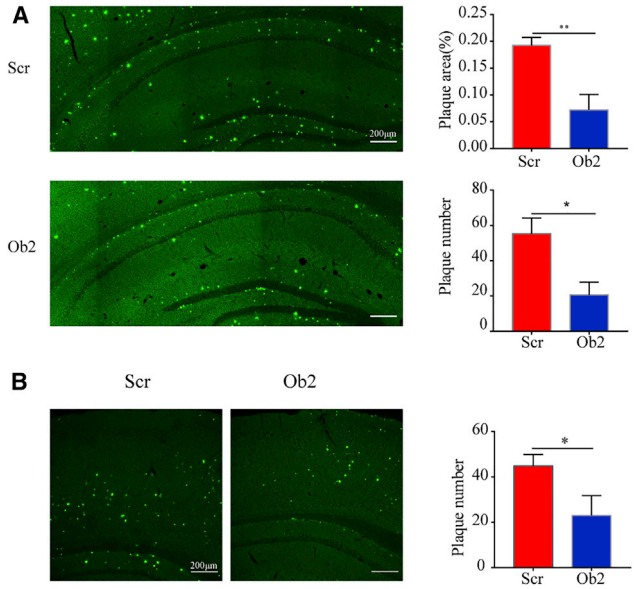

Figure 5. Plaque loaded in mouse hippocampus and cortex after administration of aptamer Ob2 and Scr

(A) Representative images (left) and quantification (right) of amyloid plaques by thioflavin-S in the hippocampus. Scale bar: 200 μm. **p < 0.01, *p < 0.05.

(B) Representative images (left) and quantification (right) of amyloid plaques by thioflavin-S in the cortex. Scale bar, 200 μm. *p < 0.05. (Scr: n = 5, Ob2: n = 5)

was terminated with 50 μL of stop solution 2 M H_2SO_4, and the absorbance was measured at 450 nm in a Victor X32,030 multilabel plate reader (PerkinElmer). Apparent equilibrium dissociation constant (K_d) values were determined for each aptamer by use of nonlinear regression in GraphPad Prism 7.0 software.

Repeated intraventricular infusion

A brain infusion cannula system (Ruiwode, Shenzhen, China) was implanted via right intracerebroventricular injection of 4-month-old male 5×FAD mice as described previously.[41] Briefly, mice were anesthetized with 4% chloral hydrate (0.2 mL per 20 g) and then fixed in stereotactic apparatus (Ruiwode) until the skull of the mice was kept parallel with the table top. After creation of a middle skin incision (0.5 cm around bregma) in the cranial skin, a cannula system was implanted in the right cerebral ventricle of the mice. The coordinates were as follows: anteroposterior, 0.16 mm behind bregma; lateral, 0.8 mm from midline; and depth, 2.3 mm from skull surface. To ensure accurate positioning of the implanted cannula, mouse brain tissues were cut at 300 μm using a VT-1200S vibratome (Leica, Wetzlar, Germany), and the residual cannula traces were investigated. After implantation, the cannula was secured with dental cement, and the cap was inserted into the cannula to prevent occlusion and infection. Mice were randomly divided into the Ob2 group and the Scr group. The Scr group was marked with color in the dental cement with marker pen. After sufficient awakening from anesthesia, mice were housed two per cage with a clapboard for 3–4 days. Then, aptamer Ob2 or Scr was administered using a four-channel drug pump (Shenzhen Ruiwode Life Technology Co., Ltd). The aptamer was administered a total of 15 times at a frequency of once every 3 days and a total dose of 0.4 nmol per injection.

Open-field test

The open-field test (OFT) is widely used to evaluate locomotor activity and anxiety-like behavior in mice.[42] Mice were gently and individually placed into the center of an open-field apparatus consisting of a square arena (60 × 60 × 40 cm). The behavior of the mice was then recorded for 5 min using an automated video tracking system. After each trial, the apparatus was thoroughly cleaned with paper towel with 70% ethanol. The DigBehv animal behavior analysis program allowed for the calculation of parameters including total distance traveled and relative time spent in the center versus the periphery.

Y maze test

The spontaneous alternation Y maze test allows us to assess spatial working memory that is dependent on the hippocampus and was performed as described previously.[41] The experimental apparatus was made from black Plexiglas and consisted of three black 35 × 5 × 10 cm arms separated by 120°. Before and after each trial, the apparatus was cleaned with 70% ethanol and allowed to dry. Each mouse was placed at the end of one arm and allowed to move freely through the maze during an 8-min session. An arm entry occurred when all four paws of the mouse had been completely placed in the arm. The sequence and total number of arms entered were recorded using a video camera. A spontaneous alternation was defined as entry into a different arm in each of three consecutive arm entries, for example, ABC, BAC, or ACB, but not CAA. The percentage of the alternation was used to estimate short-term memory, and total arm entries were used as an indicator of locomotor activity. Then, the percentage of spontaneous alternation was calculated using the following formula:

$$\%\text{Alternation} = (\text{Number of alternations}) \times /(\text{Total arm entries} - 2) \times 100$$

Morris water maze test

The Morris water maze test is widely used to assess spatial learning and retrieval learning.[43] The test was conducted in a round pool 1.2 m in diameter, and the pool was filled with water supplemented with opaque, white, nontoxic water-soluble paint. The temperature of the pool was maintained at 22 ± 1°C. The pool was divided into four quadrants of equal area, and a black platform (10 cm in diameter) was placed 1 cm below the surface of the water and was invisible to the mice. Several prominent visual cues were fixed at distinct positions around the pool. All mice were subjected to one session of four trials daily using each of the four start positions once each day for over 5 consecutive days. For each trial, the mouse was placed in the water facing the wall of the pool at one of four starting points, excluding the quadrant with the platform. The order of these

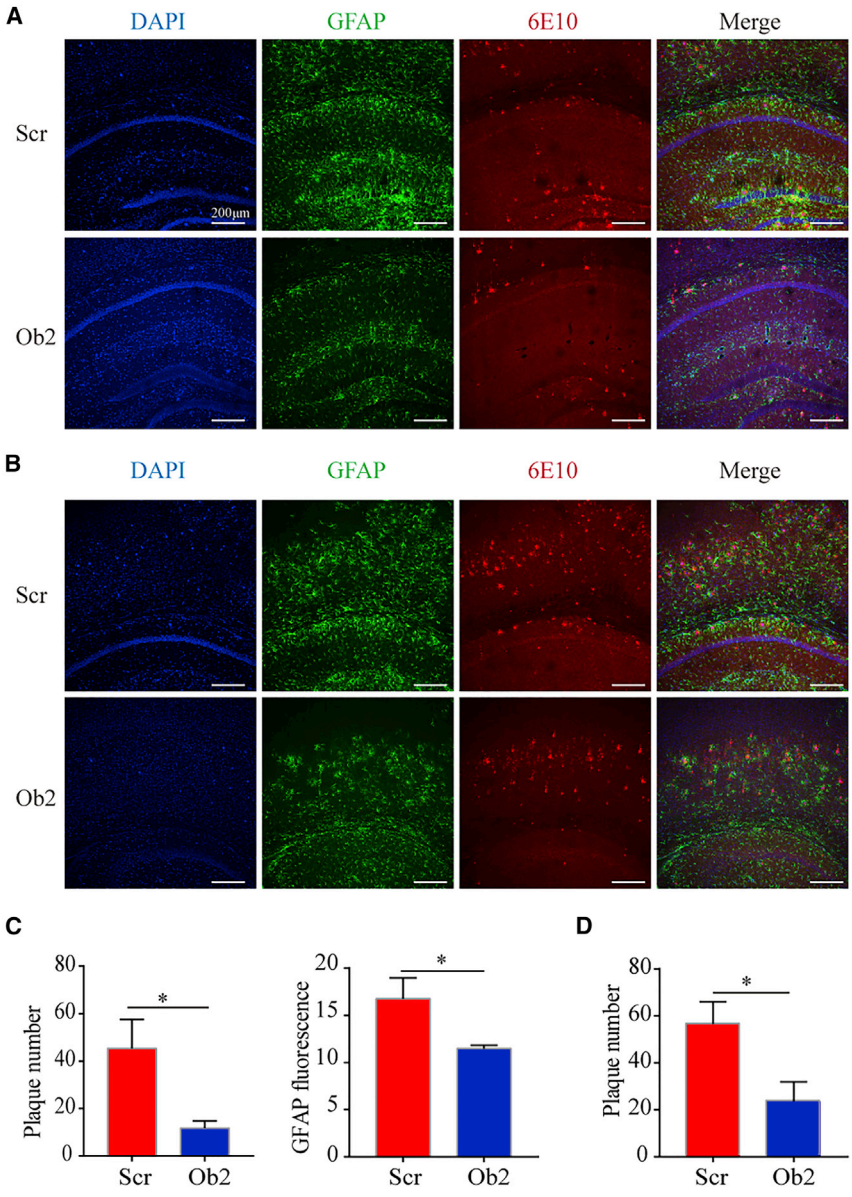

Figure 6. Immunofluorescence staining of the hippocampus and cortex in mice after intracerebral administration of aptamers Ob2 and Scr

(A) Confocal images of nuclei (DAPI, blue) GFAP (green), and 6E10 (targeting Aβ, red) in the hippocampal slices. Scale bar, 200 μm.

(B) Confocal images of nuclei (DAPI, blue) GFAP (green), and 6E10 (targeting Aβ, red) in the cortical slices. Scale bar, 200 μm.

(C) The 6E10-positive plaque number and GFAP fluorescence in the hippocampus. *$p < 0.05$.

(D) The 6E10-positive plaque number in the cortex. *$p < 0.05$. (Scr: n = 5, Ob2: n = 5). The images of Figures 6A and 6B are from the same sample.

starting points was determined randomly or semirandomly for each trial and changed each day, but the location of the escape platform remained in the same quadrant during the entire experiment. The movement of the mice was recorded with the help of video cameras and connected to a computerized video tracking system. During training days (spatial acquisition phase), all mice were given a 90-s trial to locate the hidden platform. Mice that failed to locate the platform within the time limit were guided to it and allowed to rest for 30 s. The goal of the training was to help the mice learn how to locate the hidden platform from different starting points and orientations. On the testing day, the platform was removed and the time spent in the platform quadrant and the number of platform crossings were recorded during a 60-s period.

Brain sample preparation

One day after the end of the behavioral tests, mice were anesthetized by intraperitoneal injection of chloral hydrate as described above. Each group was divided into approximately one-half for perfusion and the other half for brain lysate. Perfusion was performed by intracardiac puncture with 0.9% saline solution to eliminate blood followed by ice-cold 4% paraformaldehyde in 0.1 M phosphate buffer. The brains were removed and bisected and then postfixed overnight in 4% paraformaldehyde in 0.1 M phosphate buffer. After the brains were immersed in 30% sucrose for 48 h for cryoprotection, brain tissues were cut into 35-μm sections using a Leica CM1950 cryostat (Leica Biosystems, Wetzlar, Germany) with Tissue-Tek OCT at −20°C. One part of the brain tissue sections was used for ThS staining, and the other part was used for IHC. For brain lysates, brains were divided in half down the midline for ELISA and western blot (WB). The cerebral hemispheres were removed, and the hippocampal and cortical regions were dissected. Tissues were then homogenized in ice-cold RIPA lysis buffer (P89901, Thermo Fisher Scientific) containing 1× protease inhibitors (P1862209, Thermo Fisher Scientific) for WB and in 8 volumes of cold 5 M guanidine-HCl per 100 mg brain tissue in 50 mM Tris for ELISA.

Western blotting

Brain tissue lysates for WB were incubated on ice for 30 min and centrifuged at 12,000 × *g* for 20 min at 4°C. The protein concentration in the supernatant was quantified using a BCA assay kit (23,227, Thermo Fisher Scientific). Equal amounts of protein (20 μg) in the supernatant were separated by 8% SDS-PAGE gel, and proteins were then transferred to a polyvinylidene difluoride (PVDF) membrane (Millipore, Bedford, MA) after electrophoresis. The membrane was blocked with 5% nonfat dried milk at RT for 1.5 h, followed by incubation with primary antibodies against sAPPβ, sAppα (IBL, Fujioka,

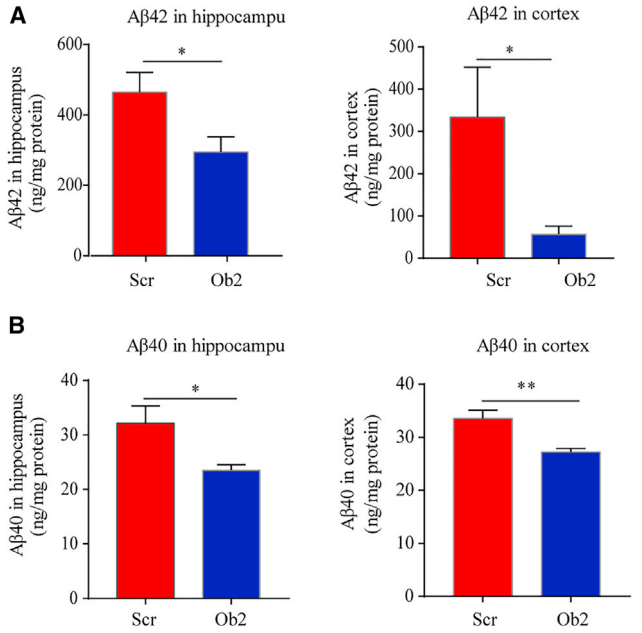

Figure 7. Total levels of $A\beta_{42}$ and $A\beta_{40}$ in the mouse cortex and hippocampus after administration of aptamers Ob2 and Scr

(A) Total $A\beta_{42}$ levels in hippocampus and cortex. *$p < 0.05$.

(B) Total $A\beta_{40}$ levels in hippocampus and cortex. **$p < 0.01$, *$p < 0.05$. (Scr: n = 5, Ob2: n = 5)

Japan), BACE-1 (Abcam, Cambridge, MA), GFAP (Millipore, Burlington, MA, USA), and β-actin (Boster, Wuhan, China) as control proteins at 4°C overnight. After three washes with 1× TBST, the membrane was incubated in horseradish peroxidase-conjugated secondary antibody (ZSGB-BIO, Beijing, China) at RT for 1 h. Membranes were incubated in Clarity Western ECL Substrate (Bio-Rad, Hercules, CA, USA), and visualized with the Gel Doc XR System (Bio-Rad) and analyzed using AlphaEaseFC software.

Enzyme-linked immunosorbent assay

Brain tissue lysates after homogenization for ELISA were then incubated on a shaker at RT for 3 h and diluted with 10-fold cold PBS containing 1× protease inhibitor cocktail. The homogenates were centrifuged at 16,000 × *g* for 20 min. The supernatants were collected, and the concentrations of Aβ ($A\beta_{40}$ or $A\beta_{42}$) were detected by specific ELISA kits (Invitrogen, Carlsbad, CA, USA) according to the manufacturer's instructions.

Thioflavin-S staining

ThS staining was used to observe senile plaques in the hippocampus and cortex and was performed as described previously.[41] After a wash with PBS for 30 min, brain slices were stained in freshly prepared 0.01% solution of ThS with 50% alcohol for 8 min in the dark. Then, slices were washed twice in 50% alcohol for 5 min each time and subsequently washed twice in PBS for 5 min each time. After mounting, image acquisition was performed under a confocal laser scanning microscope (Leica, Mannheim, Germany).

Immunohistochemistry

The brain slices were gently washed three times in PBS prior to blocking with 5% BSA and 0.3% Triton X-100 in PBS for 1 h. Sections were then incubated overnight in a solution containing antibodies against either anti-Aβ 6E10 (BioLegend, San Diego, CA, USA) or anti-GFAP (Millipore) prepared in PBS. After three washes in PBS for 10 min each time, sections were incubated with fluorescent secondary antibodies for 1 h in the dark and washed again as previously described in PBS. Then, all sections were placed on slides, mounted with VECTASHIELD Antifade Mounting Medium with DAPI (Vector Laboratories, Burlingame, CA, USA) and scanned with a confocal laser scanning microscope (Leica, Mannheim, Germany).

Statistical analysis

Statistical analyses were performed with GraphPad Prism version 7.0 (GraphPad Software). All data are expressed as the mean ± SEM. Statistically significant differences between groups were determined using Student's t test or one-way ANOVA. A value of $p < 0.05$ was considered statistically significant. All experiments were performed at least three times.

SUPPLEMENTAL INFORMATION

Supplemental information can be found online at https://doi.org/10.1016/j.omtn.2022.02.018.

ACKNOWLEDGMENTS

This work was supported by grants from the National Natural Science Foundation of China (nos. 82073340, 81871418, 81471388), the Medical Scientific Research Foundation of Guangdong Province (A2020268), Key Area Research and Development Program of Guangdong Province (2018B030340001), the Science and Technology Program of Guangzhou (202007030013), and the Program for Changjiang Scholars and Innovative Research Team in University (No. IRT_16R37)

AUTHOR CONTRIBUTIONS

Xingmei Zhang and Yusheng Shi conceived the study and participated in its design and coordination. Zhiman Liang performed acetylcholinesterase activity assay. Zhiman Liang conducted intraventricular infusion with the help of Hongjie Luo and Yajun Chen. Zhiman Liang and Hongjie Luo conducted the behavioral tests and analysis with the help of Xin Li, Xiaoting Luo, and Yajun Chen. Zhiman Liang, Xiaoting Luo, and Mingliang Cai performed the binding affinity assay and data analyses. Zhiman Liang, Xiaoting Luo, and Yingying Fang performed the ELISA and western blot experiments and data analysis. Zhiman Liang and Ting Guo performed thioflavin-S staining and IHC analyses. Zhiman Liang and Xingmei Zhang drafted and revised the manuscript. All authors read and approved the final version of the manuscript.All authors take responsibility for the integrity of the work.

DECLARATION OF INTERESTS

The authors declare that they have no conflicts of interest.

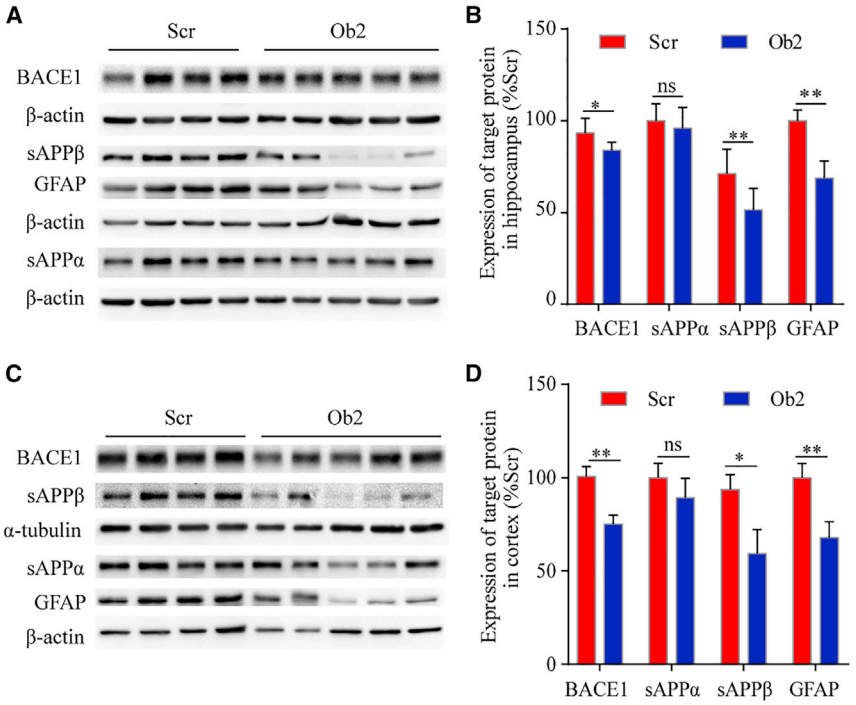

Figure 8. Expression of related proteins in 5×FAD mice after intracerebral administration of aptamers Ob2 and Scr

(A) Immunoreactive bands for secretases involved in the APP cleavage of BACE1, and its metabolites sAPPα and sAPPβ and glial fibrillary acidic protein (GFAP)-positive astrocytes in the hippocampus quantified and expressed as the percentage of Scr-treated 5×FAD levels. $^{**}p < 0.01$, $^{*}p < 0.05$, ns: no significance.

(B) Western blot analysis of hippocampal lysates from aptamer Ob2- and Scr-treated 5×FAD mice. $^{**}p < 0.01$, $^{*}p < 0.05$; ns, no significance.

(C) Immunoreactive bands for secretases involved in the APP cleavage of BACE1 and its metabolites sAPPα and sAPPβ and glial fibrillary acidic protein (GFAP)-positive astrocytes in the cortex quantified and expressed as the percentage of Scr-treated 5×FAD levels.

(D) Western blot analysis of cortex lysates from aptamer Ob2- and Scr-treated 5×FAD mice. $^{**}p < 0.01$, $^{*}p < 0.05$.

REFERENCES

1. Patterson, C. (2018). World Alzheimer Report 2018 (London: Alzheimer's Disease International).
2. Jagust, W. (2018). Imaging the evolution and pathophysiology of Alzheimer disease. Nat. Rev. Neurosci. *19*, 687–700.
3. Reiss, A.B., Arain, H.A., Stecker, M.M., Siegart, N.M., and Kasselman, L.J. (2018). Amyloid toxicity in Alzheimer's disease. Rev. Neurosci. *29*, 613–627.
4. Naseri, N.N., Wang, H., Guo, J., Sharma, M., and Luo, W. (2019). The complexity of tau in Alzheimer's disease. Neurosci. Lett. *705*, 183–194.
5. Breijyeh, Z., and Karaman, R. (2020). Comprehensive review on Alzheimer's disease: causes and treatment. Molecules *25*, 5789.
6. Calsolaro, V., and Edison, P. (2016). Neuroinflammation in Alzheimer's disease: current evidence and future directions. Alzheimers Dement *12*, 719–732.
7. Stanciu, G.D., Luca, A., Rusu, R.N., Bild, V., Beschea Chiriac, S.I., Solcan, C., Bild, W., and Ababei, D.C. (2019). Alzheimer's disease pharmacotherapy in relation to cholinergic system involvement. Biomolecules *10*, 40.
8. Haam, J., and Yakel, J.L. (2017). Cholinergic modulation of the hippocampal region and memory function. J. Neurochem. *142*, 111–121.
9. Hampel, H., Mesulam, M.M., Cuello, A.C., Farlow, M.R., Giacobini, E., Grossberg, G.T., Khachaturian, A.S., Vergallo, A., Cavedo, E., Snyder, P.J., et al. (2018). The cholinergic system in the pathophysiology and treatment of Alzheimer's disease. Brain *141*, 1917–1933.
10. Ferreira-Vieira, T.H., Guimaraes, I.M., Silva, F.R., and Ribeiro, F.M. (2016). Alzheimer's disease: targeting the cholinergic system. Curr. Neuropharmacol. *14*, 101–115.
11. Lazarevic-Pasti, T., Leskovac, A., Momic, T., Petrovic, S., and Vasic, V. (2017). Modulators of acetylcholinesterase activity: from Alzheimer's disease to anti-cancer drugs. Curr. Med. Chem. *24*, 3283–3309.
12. Wang, H., and Zhang, H. (2018). Reconsideration of anticholinesterase therapeutic strategies against Alzheimer's disease. ACS Chem. Neurosci. *10*, 852–862.
13. Ahmed, T., Zahid, S., Mahboob, A., and Mehpara Farhat, M. (2017). Cholinergic system and post-translational modifications: an insight on the role in alzheimer's disease. Curr. Neuropharmacol. *15*, 480–494.
14. Zhang, Y., Lai, B.S., and Juhas, M. (2019). Recent advances in aptamer discovery and applications. Molecules *24*, 941.
15. Ni, S., Zhuo, Z., Pan, Y., Yu, Y., Li, F., Liu, J., Wang, L., Wu, X., Li, D., Wan, Y., et al. (2020). Recent progress in aptamer discoveries and modifications for therapeutic applications. ACS Appl. Mater. Inter. *13*, 9500–9519.
16. Zhu, G., and Chen, X. (2018). Aptamer-based targeted therapy. Adv. Drug Deliv. Rev. *134*, 65–78.
17. Morita, Y., Leslie, M., Kameyama, H., Volk, D.E., and Tanaka, T. (2018). Aptamer therapeutics in cancer: current and future. Cancers *10*, 80.
18. Yan, J., Xiong, H., Cai, S., Wen, N., He, Q., Liu, Y., Peng, D., and Liu, Z. (2019). Advances in aptamer screening technologies. Talanta *200*, 124–144.
19. Wang, T., Chen, C., Larcher, L.M., Barrero, R.A., and Veedu, R.N. (2019). Three decades of nucleic acid aptamer technologies: lessons learned, progress and opportunities on aptamer development. Biotechnol. Adv. *37*, 28–50.
20. Han, J., Gao, L., Wang, J., and Wang, J. (2020). Application and development of aptamer in cancer: from clinical diagnosis to cancer therapy. J. Cancer *11*, 6902.
21. Filippi, L., Bagni, O., and Nervi, C. (2020). Aptamer-based technology for radionuclide targeted imaging and therapy: a promising weapon against cancer. Expert Rev. Med. Dev. *17*, 751–758.
22. Nimjee, S.M., White, R.R., Becker, R.C., and Sullenger, B.A. (2017). Aptamers as therapeutics. Annu. Rev. Pharmacol. Toxicol. *57*, 61–79.
23. Zhang, X.M., Li, Q., Shi, Y.S., Wu, J.H., Shao, N.S., Liu, G., and Sun, M.J. (2003). Specific oligobodies against human brain acetylcholinesterase. Brain Res. *989*, 147–151.
24. Chen, Y., Shi, G.W., Liang, Z.M., Sheng, S.Y., Peng, L., Wang, Y.P., Wang, F., and Zhang, X.M. (2019). Resveratrol improves cognition and decreases amyloid plaque formation in Tg6799 mice. Mol. Med. Rep. *19*, 3783–3790.

25. Panek, D., Wichur, T., Godyń, J., Pasieka, A., and Malawska, B. (2017). Advances toward multifunctional cholinesterase and β-amyloid aggregation inhibitors. Future Med. Chem. *9*, 1835–1854.

26. Selkoe, D.J., and Hardy, J. (2016). The amyloid hypothesis of Alzheimer's disease at 25 years. EMBO Mol. Med. *8*, 595–608.

27. Guo, T., Zhang, D., Zeng, Y., Huang, T.Y., Xu, H., and Zhao, Y. (2020). Molecular and cellular mechanisms underlying the pathogenesis of Alzheimer's disease. Mol. Neurodegener. *15*, 1–37.

28. Long, J.M., and Holtzman, D.M. (2019). Alzheimer disease: an update on pathobiology and treatment strategies. Cell *179*, 312–339.

29. Koelsch, G. (2017). BACE1 function and inhibition: implications of intervention in the amyloid pathway of Alzheimer's disease pathology. Molecules *22*, 1723.

30. Uddin, M.S., Kabir, M.T., Tewari, D., Mamun, A.A., Mathew, B., Aleya, L., Barreto, G.E., Bin-Jumah, M.N., Abdel-Daim, M.M., and Ashraf, G.M. (2020). Revisiting the role of brain and peripheral Aβ in the pathogenesis of Alzheimer's disease. J. Neurol. Sci. *416*, 116974.

31. Price, B.R., Johnson, L.A., and Norris, C.M. (2021). Reactive astrocytes: the nexus of pathological and clinical hallmarks of Alzheimer's disease. Ageing Res. Rev. *68*, 101335.

32. Zhao, Y., Wang, X., Wang, T., Hu, X., Hui, X., Yan, M., Gao, Q., Chen, T., Li, J., Yao, M., et al. (2011). Acetylcholinesterase, a key prognostic predictor for hepatocellular carcinoma, suppresses cell growth and induces chemosensitization. Hepatology *53*, 493–503.

33. Han, S.H., Park, J.C., Byun, M.S., Yi, Da., Lee, J.H., and Mook-Jung, I.; KBASE Research Group (2019). Blood acetylcholinesterase level is a potential biomarker for the early detection of cerebral amyloid deposition in cognitively normal individuals. Neurobiol. Aging *73*, 21–29.

34. Wilson, R.D., Van Mieghem, T., Langlois, S., and Church, P. (2021). Guideline no. 410: prevention, screening, diagnosis, and pregnancy management for fetal neural tube defects. J. Obstet. Gynaecol. Can. *43*, 124–139.

35. Cummings, J.L., Tong, G., and Ballard, C. (2019). Treatment combinations for Alzheimer's disease: current and future pharmacotherapy options. J. Alzheimers Dis. *67*, 779–794.

36. Li, Q., He, S., Chen, Y., Feng, F., Qu, W., and Sun, H. (2018). Donepezil-based multifunctional cholinesterase inhibitors for treatment of Alzheimer's disease. Eur. J. Med. Chem. *158*, 463–477.

37. Macdonald, J., Henri, J., Goodman, L., Xiang, D., Duan, W., and Shigdar, S. (2017). Development of a bifunctional aptamer targeting the transferrin receptor and epithelial cell adhesion molecule (EpCAM) for the treatment of brain cancer metastases. ACS Chem. Neurosci. *8*, 777–784.

38. Li, X., Yang, Y., Zhao, H., Zhu, T., Yang, Z., Xu, H., Fu, Y., Lin, F., Pan, X., Li, L., et al. (2020). Enhanced in vivo blood–brain barrier penetration by circular tau-transferrin receptor bifunctional aptamer for tauopathy therapy. J. Am. Chem. Soc. *142*, 3862–3872.

39. Ren, X., Zhao, Y., Xue, F., Zheng, Y., Huang, H., Wang, W., Chang, Y., Yang, H., and Zhang, J. (2019). Exosomal DNA aptamer targeting α-synuclein aggregates reduced neuropathological deficits in a mouse Parkinson's disease model. Mol. Ther. Nucleic Acids *17*, 726–740.

40. Ellman, G.L., Courtney, K.D., Andres, V., Jr., and Feather-Stone, R.M. (1961). A new and rapid colorimetric determination of acetylcholinesterase activity. Biochem. Pharmacol. *7*, 88–95.

41. Liang, Z.M., Peng, Y.H., Chen, Y., Long, L.L., Luo, H.J., Chen, Y.J., Liang, Y.L., Tian, Y.H., Li, S.J., Shi, Y.S., et al. (2019). The BACE1-specific DNA aptamer A1 rescues amyloid-β pathology and behavioral deficits in a mouse model of Alzheimer's disease. Nucleic Acid Ther. *29*, 359–366.

42. Gould, T.D., Dao, D.T., and Kovacsics, C.E. (2010). The open field test. Neuromethods *83*, 1–20.

43. Vorhees, C.V., and Williams, M.T. (2006). Morris water maze: procedures for assessing spatial and related forms of learning and memory. Nat. Protoc. *1*, 848–858.